Journal of Trace Elements in Medicine and Biology 94 (2026) 127854

Contents lists available at ScienceDirect

Journal of Trace Elements in Medicine and Biology

journal homepage: www.elsevier.com/locate/jtemb

# Exposure to copper induces oxidative stress and apoptosis in human MEG-01 cells

Zhanqin Huang [a,1], Yuxuan Huang [b,1], Hongxing Chen [b], Meidie Yu [b], Zihao Zhao [b], Dongqing Zhang [c,*], Qiaoxin Zhang [c,*]

[a] Department of Pharmacology, Shantou University Medical College, Shantou, Guangdong 515041, PR China
[b] Department of Clinical Medicine, Shantou University Medical College, Shantou, Guangdong 515041, PR China
[c] Department of Laboratory Medicine, The First Affiliated Hospital of Shantou University Medical College, Shantou, Guangdong 515041, PR China

ARTICLE INFO

*Keywords:*
Copper exposure
Oxidative stress
Apoptosis
Autophagy
MEG-01 cells
Wilson disease

ABSTRACT

*Background:* Wilson disease (WD), caused by *ATP7B* mutations, leads to pathological copper accumulation. Although thrombocytopenia is often reported in patients with WD, the underlying mechanisms are complex and remain unelucidated. This study used the human megakaryoblast cell line MEG-01 to investigate how excess copper affects cellular oxidative stress and apoptosis.

*Methods:* After exposing MEG-01 cells to $CuCl_2$ for 24 h, viability was determined using a Cell Counting Kit-8 (CCK-8) assay, and intracellular ultrastructural changes were observed using transmission electron microscopy (TEM). Apoptosis was quantified using annexin V/propidium iodide (PI) staining combined with flow cytometry analysis. Reactive oxygen species (ROS) levels were analyzed by 2′,7′-dichlorodihydrofluorescein diacetate staining and flow cytometry. Malondialdehyde (MDA) and superoxide dismutase (SOD) were detected using thiobarbituric acid (TBA) and water-soluble tetrazolium 8 (WST-8) assays, respectively. The expression levels of p62 and caspase-3 proteins were evaluated using western blotting.

*Results:* Compared with the control group, $CuCl_2$ treatment of MEG-01 cells significantly inhibited the viability of cells. TEM revealed mitochondrial swelling, cristae fragmentation, and endoplasmic reticulum dilatation, indicating organelle damage. The apoptotic rate exhibited a dose-dependent increase in response to $CuCl_2$, which was paralleled by a significant upregulation in the protein levels of caspase-3 and p62. Finally, treatment of MEG-01 cells with $CuCl_2$ significantly elevated the levels of ROS and MDA. While SOD activity remained unchanged in the 10 and 20 μM $CuCl_2$ groups compared to the control, it was markedly reduced following exposure to 40 μM $CuCl_2$.

*Conclusion:* Copper exposure damages MEG-01 cells. This is likely mainly due to oxidative stress and apoptosis.

## 1. Introduction

Copper is an essential trace element in human and animal physiological systems, serving as a critical cofactor for numerous metalloenzymes, including cytochrome oxidase, superoxide dismutase (SOD), and dopamine β-hydroxylase [1]. The maintenance of appropriate intracellular copper levels using homeostatic mechanisms is crucial because both copper deficiency and excess lead to developmental defects and various diseases. Copper deficiency is associated with myelopathy, pancytopenia, cardiovascular disease, and Menkes disease [2–4]. However, the required copper level for healthy metabolism is extremely low. Thus, copper accumulation exceeding metabolic requirements or copper homeostasis disorder results in toxic effects, including immunotoxicity, hematotoxicity, pulmonary toxicity, hepatotoxicity, nephrotoxicity, and neurotoxicity [5–8].

Wilson disease (WD) is an autosomal recessive disorder characterized by a variety of mutations in the *ATP7B* gene. When *ATP7B* mutation leads to dysfunctional copper transport by ATP7B, copper becomes overaccumulated in the liver. Once this amount exceeds the hepatic storage capacity, it enters the blood in the form of free copper, affecting multiple tissues and organs. Thrombocytopenia is frequently observed in Wilson's disease (WD), although its underlying mechanisms remain

* Correspondence to: 57 Changping Road, Shantou City, Guangdong Province, China.
*E-mail addresses:* zhangdongqing1976@163.com (D. Zhang), qiaoxinzhang@126.com (Q. Zhang).
[1] Zhanqin Huang and Yuxuan Huang are the co-first author and contributed equally to this study

https://doi.org/10.1016/j.jtemb.2026.127854
Received 21 July 2025; Received in revised form 26 February 2026; Accepted 2 March 2026
Available online 3 March 2026

complex and not fully elucidated [9–16]. Some studies attribute it to hypersplenism or adverse effects of penicillamine treatment [14,15]. Additionally, copper deficiency itself which can occur during WD treatment may lead to pancytopenia [3,16]. Supporting this clinical relevance, Hoagland et al. reported that 52% of WD patients presented with thrombocytopenia and 30% with leukopenia. Notably, among thrombocytopenic patients, 24 individuals did not have splenomegaly, underscoring that mechanisms beyond hypersplenism are involved [17]. To date, the precise mechanism is still incompletely understood. Given previous findings indicating that copper can induce oxidative stress and apoptosis in various tissues [18,19], we hypothesized that copper overload exerts cytotoxic effects on megakaryocytes through reactive oxygen species (ROS)-mediated organelle damage and caspase-dependent apoptosis. To test this hypothesis, we employed human MEG-01 cells as an experimental model.

## 2. Methods

### 2.1. Preparation of $CuCl_2$ solution

Copper chloride ($CuCl_2{\cdot}2\ H_2O$, 203149; Sigma, St Louis, MO, USA) was selected as the copper source. The preparation process of copper solution as follows: $CuCl_2{\cdot}2\ H_2O$ was dissolved in phosphate buffered saline (PBS) to prepare 100 mM $CuCl_2$ solution, and then stored in refrigerator at 4 °C before using.

### 2.2. Cell culture

Human MEG-01 cells (CL-0498; Procell, Wuhan, China) were maintained in RPMI-1640 medium (11965–092; Gibco, Grand Island, NE, USA) supplemented with 10% fetal bovine serum (16000–044; Gibco) and 1% penicillin-streptomycin (P4333; Sigma) under standard culture conditions (37°C, 5% $CO_2$).

### 2.3. Cell viability assay

MEG-01 cells were seeded in 96-well plates at a density of $1 \times 10^4$ cells/well and treated with $CuCl_2$ (0, 5, 10, 20, 40 and 80 μM) for 24 h, the concentration ranges of $CuCl_2$ were established to cover the range of copper concentrations found in human blood (10–40 μM). Following this treatment, 10 μL of Cell Counting Kit-8 (CCK-8; C0037; Beyotime, Shanghai, China) reagent was added to each well. The cells were then incubated for an additional 2 h at 37 ∘C, and the absorbance values were subsequently measured at 450 nm using a microplate reader (Eon, BioTek Instruments, Winooski, VT, USA).

### 2.4. Transmission electron microscopy (TEM)

The cells underwent ultrastructural analysis using TEM. Briefly, MEG-01 cells were seeded in 6-well plates at a density of $1 \times 10^4$ cells/well and treated with $CuCl_2$ at concentrations of 0, 10, 20, and 40 μM for 24 h. After treatment, the cells were harvested and fixed in McDowell–Trump fixative (4°C, 24 h), followed by staining with 1% osmium tetroxide (1 h, room temperature). After washing thoroughly, the cells were dehydrated through a series of graded ethanol solutions (30%, 50%, 70%, 80%, and 95%) for 15 min each, followed by 30 min in 100% ethanol. The cells were further dehydrated in 100% acetone for 10 min, followed by overnight infiltration with acetone using Spurr resin mixture (1:1). The resin was refreshed and allowed to penetrate the cells for 3 days. Finally, they were embedded overnight in pure Spurr resin at 60°C in an oven The specimen blocks were underwent ultrathin sectioning (70 nm) on an RMC PowerTomeXL ultramicrotome (Boeckeler Instruments, Inc., Tucson, AZ, USA) using a knife boat and an Ultra 45 diamond knife (Diatome, Biel, Switzerland). The sections were collected on copper grids, stained with uranyl acetate and lead citrate, and visualized using an HT7800 TEM (Hitachi, Tokyo, Japan).

### 2.5. Apoptosis analysis using flow cytometry

Flow cytometry was used to assess cellular apoptosis. An Annexin V-FITC apoptosis detection kit (C1062S; Beyotime) was used to detect apoptotic rate according to the supplier's instructions. Briefly, MEG-01 cells were treated as described above. After treatment, cells and supernatant were collected in 5 mL tubes and centrifuged at 1000 × g for 5 min, after which the supernatant was discarded. The cells were then washed twice with ice-cold phosphate-buffered saline (PBS; pH 7.4), and resuspended in 195 μL Annexin V Binding Buffer. Then, 5 μL Annexin V-FITC and 10 μL propidium iodide (PI) were added, followed by gentle vortexing and incubation in the dark (20°C–25°C, 15 min). The samples were immediately analyzed using a CytoFLEX flow cytometer (Beckman Coulter Life Sciences, California, USA) at an excitation wavelength of 488 nm. At least 10,000 cells were collected from each group, and the data were analyzed using CytExpert v2.0 software (Beckman Coulter Life Sciences), with early apoptosis defined as annexin $V^+/PI^-$ cells and late apoptosis defined as annexin $V^+/PI^+$ cells.

#### 2.5.1. Western blotting

Cells were lysed in RIPA buffer (P0013B; Beyotime) containing 1 mM phenylmethylsulfonyl fluoride and protease/phosphatase inhibitors (P1051; Beyotime). The lysates were centrifuged (12,000 × g, 10 min, 4°C), and the supernatants were collected for determination of the protein concentration using a BCA assay (P0011; Beyotime), with bovine serum albumin as the standard. Equal protein amounts (20–30 μg/lane) of each supernatant sample were resolved using electrophoresis on 10% sodium dodecyl sulfate-polyacrylamide gels (P0523S; Beyotime) at 350 mA for 60 min and transferred to polyvinylidene membranes (ISEQ00010; Millipore, Burlington, MA, USA). The membranes were blocked with 5% skim milk for 2 h at room temperature and then incubated overnight at 4°C with specific primary antibodies diluted in the corresponding blocking solution. The primary antibodies used in this study were as follows: anti-β-actin (1:3000, mouse monoclonal, AF0003; Beyotime), anti-caspase-3 (1:2000, rabbit monoclonal, AF1213; Beyotime), anti-p62 (1:2000, mouse monoclonal, AF0279; Beyotime). Following three washes (10 min each) with Western wash solution (P0023C; Beyotime), the membranes were incubated with appropriate horseradish peroxidase (HRP)-conjugated secondary antibodies (goat anti-rabbit IgG, 1:2000, A0216, Beyotime; or goat anti-mouse IgG, 1:2000, A0192, Beyotime) for 1 h at room temperature. The membranes were developed using a chemiluminescent imaging system and analyzed in grayscale with ImageJ v2 software (National Institutes of Health, Bethesda, MD, USA).

### 2.6. Detection of oxidative stress markers

The ROS levels in MEG-01 cells were detected using 2′,7′-dichlorodihydrofluorescein diacetate (DCFH-DA, S0033S; Beyotime). Briefly, DCFH-DA was diluted to a concentration of 10 μg/mL in 1 × PBS. After washing the MEG-01 cells once with 1 × PBS, they were incubated with 2 mL of the diluted DCFH-DA solution (1:1000) at 37ºC for 20 min. Subsequently, the cells were washed three times with 1 × PBS to remove any unbound dye and analyzed using flow cytometry (excitation/emission: 488/525 nm). At least 10,000 cells were collected from each group, and the data were analyzed using CytExpert v2.0 software, with the relative ROS levels expressed as the average fluorescence intensity.

Lipid peroxidation was quantified using a malondialdehyde (MDA) assay kit (S0131S; Beyotime). Cell lysates were mixed with thiobarbituric acid (TBA) and heated (95°C, 60 min). After cooling to room temperature and centrifuging to remove any precipitate, the absorbance of the supernatant was measured at 532 nm using a microplate reader (Eon, BioTek Instruments). A standard curve was generated using known concentrations of the MDA standard provided with the kit, and the MDA concentration in each sample was interpolated from this curve.

The total SOD activity was determined using a water-soluble

tetrazolium 8 (WST-8)-based SOD assay kit (S0101S; Beyotime). MEG-01 cells ($1 \times 10^6$) were pelleted (600 × g, 5 min, 4°C), washed twice with ice-cold PBS, and lysed in 100 μL of SOD sample preparation solution by gentle pipetting. After centrifugation (12,000 × g, 10 min, 4°C), the supernatant was collected for immediate assay. The WST-8/enzyme working solution was prepared fresh by mixing 151 μL of SOD detection buffer, 8 μL of WST-8, and 1 μL of enzyme solution per reaction. The 40 × reaction initiation solution was diluted 1:39 with SOD detection buffer to obtain the reaction initiation working solution. Each well contained 20 μL of sample (or buffer for blanks), 160 μL of WST-8/enzyme working solution, and 20 μL of reaction initiation working solution. Two control wells were included: Blank 1 (buffer instead of sample) and Blank 2 (without reaction initiation solution). The plate was incubated at 37°C for 30 min in the dark, and absorbance was measured at 450 nm using a microplate reader (Eon, BioTek Instruments). The inhibition rate was first calculated using the formula: Inhibition Rate(%) $= (A_{blank1} - A_{sample})/(A_{blank1}\text{-}A_{blank2}) \times 100(\%)$, where $A_{blank1}$ represents the maximum absorbance in the absence of sample, $A_{blank2}$ represents the background absorbance without the reaction initiation solution and test sample, and $A_{sample}$ is the absorbance of the test sample. SOD activity was then calculated from the inhibition rate using the formula provided by the manufacturer: SOD Activity (units) = Inhibition Rate (%) / [1 – Inhibition Rate (%)]. One unit of SOD was defined as the amount of enzyme that inhibits the superoxide-driven reaction by 50% under the assay conditions.

### 2.7. Statistical analysis

Data were analyzed using SPSS v26.0 statistical software (SPSS Inc., Chicago, IL, USA). All results were expressed as the mean ± standard deviation (SD). Statistical differences between groups were compared using *t*-test or one-way analysis of variance. *P*-values $< 0.05$ were considered statistically significant. All experiments were conducted in triplicate for accuracy and reproducibility.

## 3. Results

### 3.1. Effect of copper exposure on cell viability

The data presented in Fig. 1 show a dose-dependent effect of $CuCl_2$ on the viability of MEG-01 cells across the tested concentration range (0, 5, 10, 20, 40, and 80 μM). As there was no significant difference in cell viability between the 5 μM group and the control group, while viability in the 80 μM group dropped markedly to 36%, concentrations of 0, 10, 20, and 40 μM were selected for subsequent experiments.

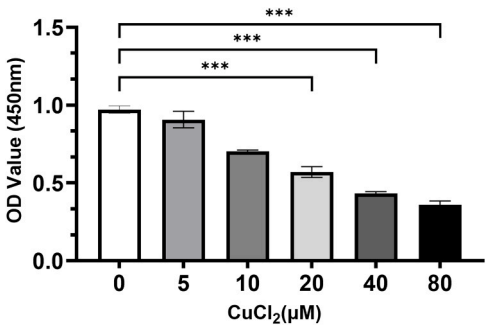


**Fig. 1. Evaluation of MEG-01 cell viability using the CCK-8 assay.** Values are expressed as the mean±SD. The treatment groups were compared with the control group (0 μM $CuCl_2$) to calculate relative ratios (***$P < 0.001$ vs. Control, n = 3).

### 3.2. Copper-induced ultrastructural alterations in MEG-01 cells

TEM was used to observe ultrastructural changes in MEG-01 cells exposed to varying concentrations of $CuCl_2$. The structure of the mitochondria and endoplasmic reticulum (ER) was intact in the control group. After exposure to 10 μM $CuCl_2$ for 24 h, mild mitochondrial swelling and partial cristae fragmentation were observed, along with partial ER fragmentation. Increasing concentrations of $CuCl_2$ led to more severe mitochondrial swelling, cristae fragmentation, vacuolation, and ER dissolution, particularly in the 40 μM $CuCl_2$ group, where autophagosomes were observed (Fig. 2). These findings indicated progressive copper-induced organelle damage.

### 3.3. Copper exposure induced apoptosis of MEG-01 cells

MEG-01 cells were treated with 0, 10, 20, and 40 μM $CuCl_2$ for 24 h. Following annexin V-FITC/PI staining, the apoptosis rate was detected by flow cytometry. Exposure to 10, 20, and 40 μM $CuCl_2$ resulted in apoptosis rates of 9.41%, 11.38% and 13.5%, respectively, which were significantly higher than the control group (6.69%, $p < 0.01$), indicating a dose-dependent effect (Fig. 3a-b). These findings demonstrated that apoptosis induction was gradually enhanced with increased $CuCl_2$ levels in the cell culture system. Furthermore, Western blotting revealed upregulated p62 and caspase-3 levels, which are key markers of autophagic flux and apoptosis (Fig. 3c–d).

### 3.4. Copper exposure induced oxidative stress in MEG-01 cells

To assess the intracellular concentration of oxygen radicals, we quantified the ROS levels in MEG-01 cells following $CuCl_2$ exposure. ROS levels were significantly increased in the 10 and 20 μM $CuCl_2$ groups compared with the control group ($P < 0.001$). However, in the 40 μM $CuCl_2$ group, although the ROS level was higher than that of the control group ($P < 0.001$), it was significantly decreased compared with the 10 and 20 μM $CuCl_2$ groups ($P < 0.001$; Fig. 4a). Changes in MDA levels were consistent with those of ROS (Fig. 4b). The activity of SOD, a key antioxidant enzyme, was only slightly increased in the 10 and 20 μM $CuCl_2$ groups, and the difference was not significant compared with the control group. However, the SOD concentration in the 40 μM $CuCl_2$ group was significantly lower than that in the control group ($P < 0.001$; Fig. 4c).

## 4. Discussion

Copper homeostasis is crucial for maintaining normal cellular functions and physiological processes. Excessive copper accumulation leads to overproduction of reactive oxygen species, causing cellular damage and even death. Although numerous studies have investigated the cytotoxicity of copper, only a limited number have specifically addressed its toxic effects on hematopoietic cells. For instance, Tao et al. found that $CuSO_4$ induces structural and functional alterations in erythrocytes via oxidative stress, including disruption of membrane integrity, changes in fluidity and osmotic fragility, and reduced ATPase-mediated energy supply, ultimately leading to hemolysis in goat red blood cells [20]. Sadiq et al. reported that copper nanoparticles (15 mg/kg) significantly affected reticulocyte frequency and caused DNA damage in the bone marrow cells of male BALB/c mice [21]. Two additional studies demonstrated that copper nanoparticles can alter hematological parameters and induce morphological changes in rat bone marrow [22,23], further supporting the cytotoxic impact of copper exposure on bone marrow cells. Nevertheless, the specific effects of copper on megakaryocytes remain unexplored.

MEG-01 cells, a human megakaryoblast leukemia cell line, is a popular cell line used for studying megakaryocyte maturation and platelet-like particle formation. Similar to natural megakaryocytes development and maturation, MEG-01 cells display phenotypic

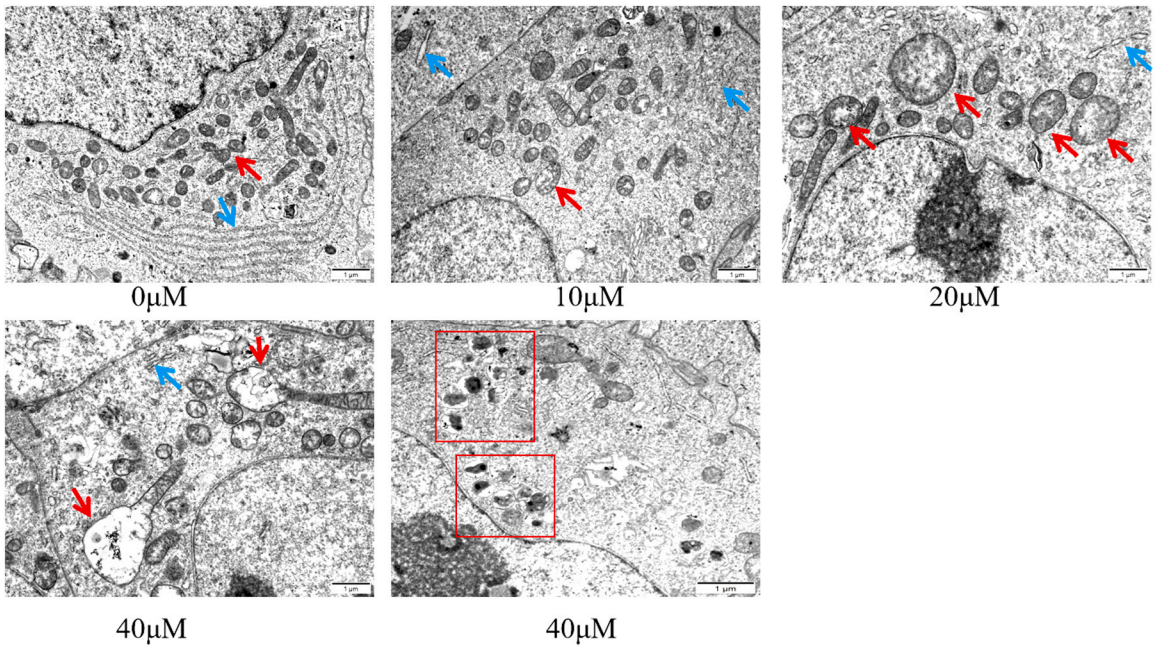


**Fig. 2. Ultrastructural changes in $CuCl_2$-treated MEG-01 cells** (20,000 × magnification; scale bar = 1 μm). Control group (0 μM $CuCl_2$): intact mitochondria (red arrows) and ER (blue arrows); 10 μM $CuCl_2$ group: mild mitochondrial swelling (red arrows) and partial ER dilatation (blue arrows); 20 μM $CuCl_2$ group: mitochondrial swelling, cristae fragmentation and vacuolization (red arrows), and fragmented ER (blue arrow); 40 μM $CuCl_2$ group: severe mitochondrial swelling and vacuolation (red arrows), fragmented ER (blue arrow), and autophagosomes (red square circle).

properties that closely resemble their natural counterparts as they mature including increasing in size, producing membranous extensions, increasing DNA content, and the production of functional platelet-like particles [24]. Thus, we established an in vitro model of copper-exposed MEG-01 cells to investigate the effect of copper on megakaryocytes. Cell viability is a crucial indicator of the cytotoxic effects of copper. When MEG-01 cells were exposed to different concentrations of copper for 24 h, the viability decreased and the apoptosis rate increased in a dose-dependent manner. Besides, observation of the ultrastructure of MEG-01 cells using TEM revealed that the mitochondria and ER suffered varying degrees of damage, including mitochondrial vacuolation, cristae swelling and rupture, and ER dilatation and dissolution. These presentations showed that exposure to excessive levels of copper was toxic to MEG-01 cells.

Several pathways have been implicated in the molecular mechanisms of copper toxicity, including oxidative stress, apoptosis, autophagy, ferroptosis and the recently proposed cuproptosis [18,19,25,26]. A well-established pathway is the induction of profound oxidative stress. In recent years, many studies have examined the induction of oxidative stress by excessive copper in various cells and tissues [27–30]. In addition, it has been reported that certain antioxidant agents can mitigate the damage caused by copper deposition in target cells or tissues through the inhibition of oxidative stress [31–33]. For example, Pandey et al. reported that melatonin protects ATP7B−/− HepG2 cells from copper-induced apoptosis by alleviating mitochondrial oxidative stress. In vivo studies also demonstrated that melatonin treatment reduced copper-induced oxidative stress in zebrafish embryos. These findings clarify the crucial role of oxidative stress in copper toxicity and provide a basis for developing antioxidant-based therapies [31].

Oxidative stress arises from an imbalance between cellular oxidative and antioxidant systems, primarily due to excessive production of free radicals and related ROS. Desaulniers et al. demonstrated that exposure of HC-04 human liver cells to $CuCl_2$ (100–200 μM) for as little as 3 h significantly increased ROS levels [34]. In our study, we likewise observed a marked rise in ROS in MEG-01 cells after 24 h of exposure to relatively low concentrations of $CuCl_2$ (10–40 μM). However, certain studies suggest that under physiologically relevant conditions, copper may preferentially bind to and deplete thiol compounds such as glutathione, rather than directly generating substantial hydroxyl radicals via the Fenton reaction. This implies that in some contexts, oxidative stress manifested as glutathione (GSH) depletion could be the primary driver of copper toxicity, with ROS generation possibly being a downstream or concomitant event [35]. Furthermore, the recently elucidated mechanism of cuproptosis reveals that excess copper can directly bind to lipoylated tricarboxylic acid (TCA) cycle proteins, leading to their aggregation, proteotoxic stress, and subsequent cell death [26]. In this pathway, ROS production may occur as a concomitant outcome of mitochondrial dysfunction, rather than serving as the sole or principal initial cause of cell death. This contested aspect warrants further investigation for clarification.

ROS are involved in various cellular metabolic reactions. It may react with large biomolecules, such as DNA, RNA, and proteins, and small biomolecules, such as glutathione and unsaturated fatty acids [36]. Since MDA is the final cytotoxic product of lipid peroxidation, its levels are considered the best measure of lipid peroxidation status and cell membrane damage induced by ROS production. Our investigation revealed that after copper exposure, ROS and MDA showed similar trends in MEG-01 cells, with both gradually increasing in the 10 and 20 μM $CuCl_2$ groups, but decreasing in the 40 μM $CuCl_2$ group. These results suggest that copper stimulates MDA production through excessive ROS generation, resulting in increased lipid peroxidation products and oxidative stress in MEG-01 cells.

To assess the antioxidative capacity of the megakaryocytes in response to copper treatment, the SOD activity was investigated as marker for oxidative stress. SOD, which clears superoxide anion free radicals and is considered crucial for defending cells against ROS and protecting them from oxidative damage. The main function of SOD is the conversion of superoxide anion free radicals into oxygen or $H_2O_2$, thereby protecting cellular structural and functional integrity [37,38]. In our study, although SOD activity was slightly increased in the 10 and 20 μM $CuCl_2$ groups, no significant differences were observed compared with the control group. In contrast, SOD activity decreased in the 40 μM $CuCl_2$ group and was significantly lower than that in the control group. We hypothesized that exposure to low copper concentrations would

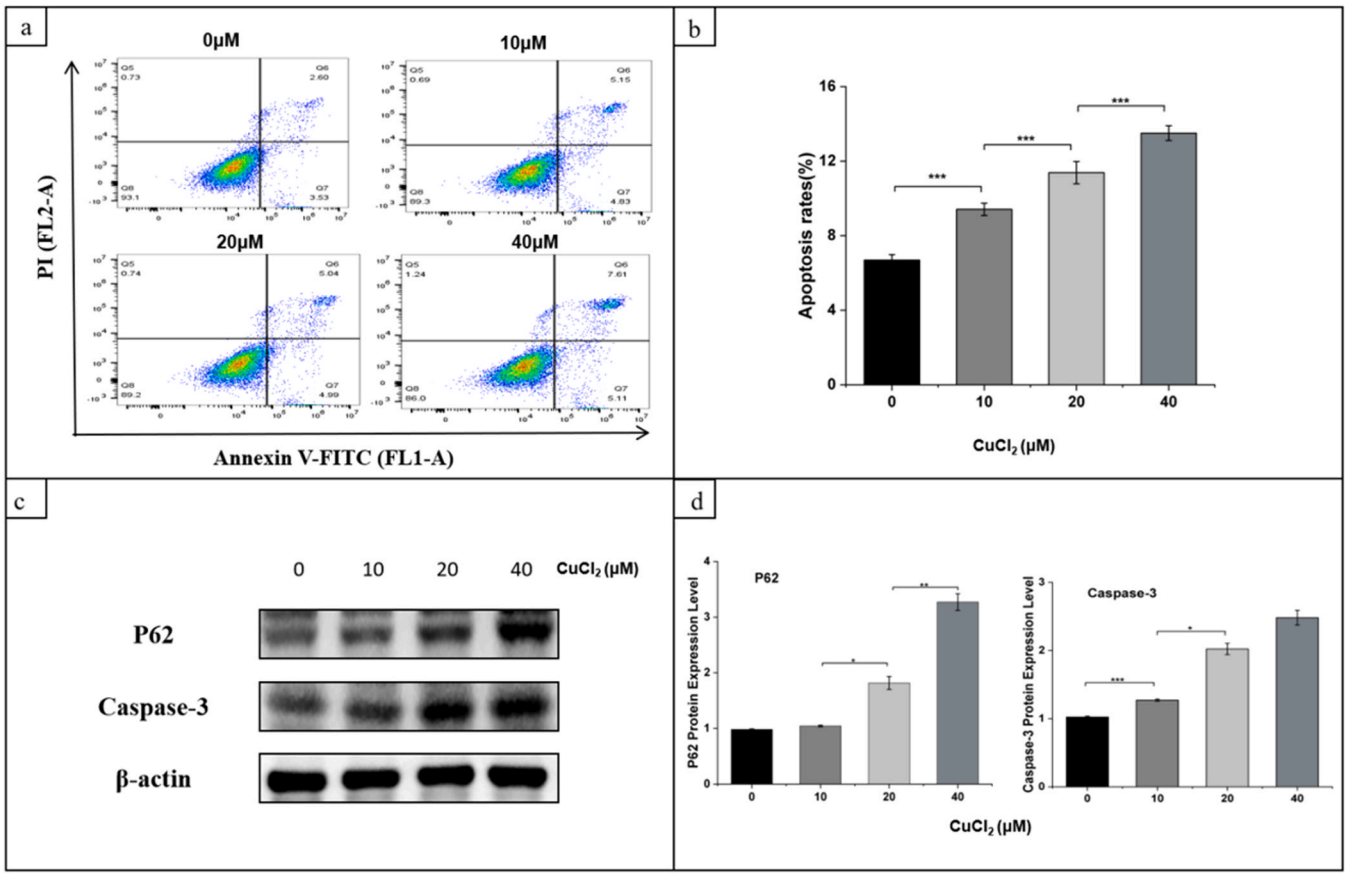


**Fig. 3. Copper-induced dysregulation of apoptosis and autophagy.** (a) Apoptosis was quantified by flow cytometry using Annexin V/PI dual staining. Cells were classified as follows: early apoptotic cells (Annexin $V^+/PI^-$), and late apoptotic cells (Annexin $V^+/PI^+$). (b) The data are presented as the percentage of total apoptotic cells (early apoptosis cells+ late apoptosis cells), and expressed as the mean ± SD. (c) Western blotting to determine the protein expression levels of p62 and caspase-3. (d) Quantitative analysis of the protein expression levels of p62 and caspase-3, data normalized to β-actin. (*$p < 0.05$, **$p < 0.01$, and ***$p < 0.001$ vs. control, n = 3).

activate the antioxidant system, however, as copper levels increase, the consumption of antioxidant molecules also rises, eventually leading to their substantial depletion.

We analyzed the expression of key proteins regulating apoptosis and autophagy. While apoptosis can be initiated by diverse stimuli, it proceeds primarily through two central pathways: the mitochondria-mediated intrinsic pathway and the death receptor-triggered extrinsic pathway. Both pathways converge on the activation of caspases [39]. Among these, caspase-3 serves as the principal effector caspase, executing apoptosis through mediation of a downstream lethal cascade. Some studies have confirmed the occurrence of apoptosis via this caspase-dependent mechanism [40–42]. In our study, exposure to $CuCl_2$ resulted in a marked increase in caspase-3 protein expression compared with the control, indicating that caspase activation contributes to copper-induced megakaryocyte apoptosis.

The molecular mechanism of autophagy involves a series of autophagy-related (Atg) proteins. A central event in this process is the conversion of microtubule-associated protein 1 light chain 3 (LC3-I) to its lipidated form, LC3-II, which is subsequently incorporated into the autophagosomal membrane [43,44]. Concurrently, p62 functions as a key scaffold and selective autophagy receptor, linking cellular stress signaling to lysosomal degradation. It simultaneously binds to ubiquitinated cargo via its C-terminal UBA (Ub-associated) domain and to LC3 on autophagosomal membranes through its LIR (LC3-interacting region) motif, thereby facilitating the autophagic clearance of protein aggregates, damaged organelles, or pathogens [45,46]. Recent studies have demonstrated that copper-induced autophagy occurs in a variety of cell types, including hepatocytes, male germ cells, mesangial cells and neuronal cells [47–51]. For instance, Tang et al. reported that CuSO4 triggered the enhanced expression of autophagy and necroptosis signaling molecules in wild-type (WT) HepG2 cells and R778L cells. Remarkably, higher levels of autophagy and necroptosis were observed in R778L cells compared with those in WT cells [48]. Similarly, Lu et al. observed that $CuSO_4$ induced a dose-dependent increase in the protein levels of Atg7, p62, and the LC3BII/LC3BI ratio in human neuroblastoma SH-SY5Y cells, with a particularly pronounced effect in the high-dose group [51]. In line with these findings, our study also revealed an upregulation of p62 along with the presence of autophagosomes in MEG-01 cells, further supporting the activation of autophagy under copper overload conditions.

## 5. Conclusion

This study aimed to investigate the effects and underlying mechanisms of copper exposure on the human megakaryoblastic cell line MEG-01, given its potential relevance to the pathogenesis of thrombocytopenia in Wilson's disease (WD) patients. Our results indicate that excessive copper exerts cytotoxic effects on MEG-01 cells, characterized by elevated levels of ROS and MDA, reduced SOD activity, upregulation of p62 and caspase-3 protein expression, and dose-dependent induction of apoptosis. Nevertheless, several limitations should be acknowledged. First, by focusing exclusively on cytotoxic concentrations, we were unable to capture early cellular responses or time-dependent adaptations to copper exposure. Second, although autophagy activation was confirmed through ultrastructural evidence and elevated p62 expression, the upstream signaling events that connect copper overload to

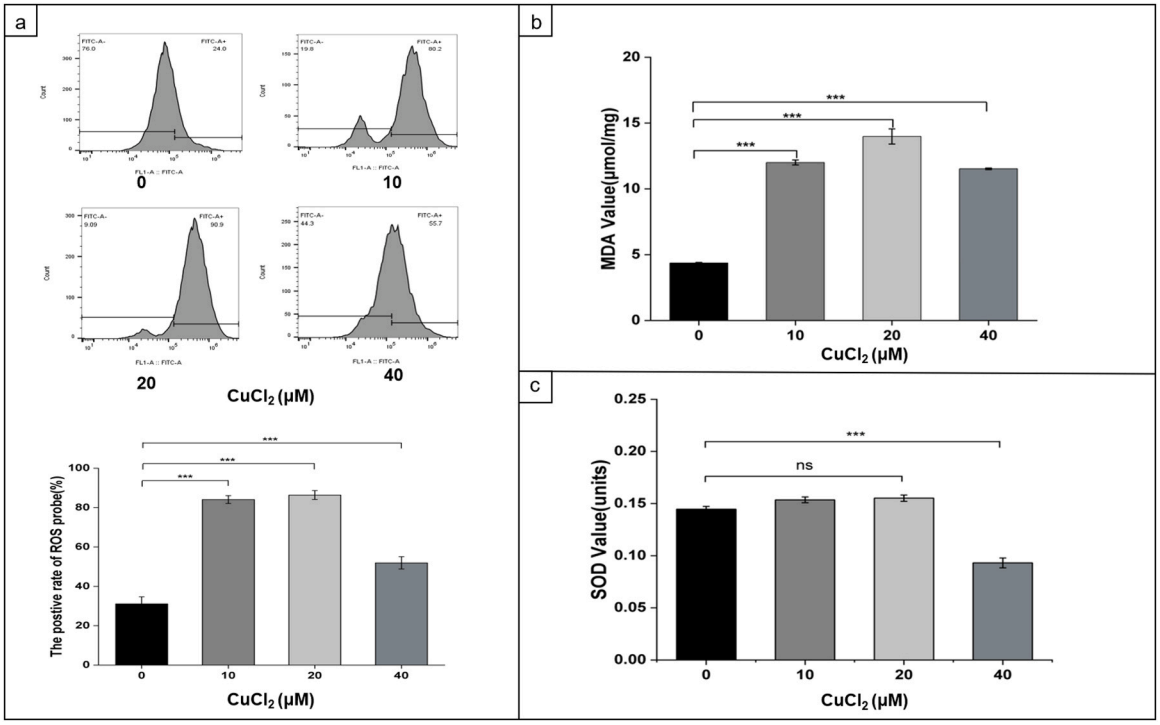


**Fig. 4. $CuCl_2$ induces oxidative stress using ROS in MEG-01 cells.** (a) ROS-positive cells. (b) MDA content. (c) SOD activity. Data are presented as the mean ± SD. (***$p < 0.001$ vs. control, n = 3).

autophagy initiation remain to be elucidated. Third, although elevated ROS levels coincided with apoptosis and autophagic activation, a causal link between copper-induced oxidative stress and these cellular processes was not functionally validated through rescue experiments. Finally, this study focused on apoptosis and autophagy, however, copper toxicity may also trigger alternative cell death modalities such as cuproptosis. Potential crosstalk or hierarchy among these pathways under copper stress warrants further investigation. Future studies will address these aspects to deepen our understanding of copper-mediated megakaryocyte injury.

## Data statement

The datasets used and analyzed during the current study are available from the corresponding author on reasonable request.

## Funding

This research did not receive any specific grant from funding agencies in the public, commercial, or not-for-profit sectors.

## CRediT authorship contribution statement

**Qiaoxin Zhang:** Writing – original draft. **Yuxuan Huang:** Formal analysis, Data curation. **Zhanqin Huang:** Investigation, Conceptualization. **Meidie Yu:** Investigation, Formal analysis, Data curation. **Hongxing Chen:** Investigation, Formal analysis, Data curation. **Dongqing Zhang:** Writing – review & editing, Writing – original draft, Formal analysis, Data curation, Conceptualization. **Zihao Zhao:** Formal analysis, Data curation.

## Declaration of Competing Interest

The authors declare that they have no known competing financial interests or personal relationships that could have appeared to influence the work reported in this paper.

## Acknowledgements

Not applicable

## References

[1] H. Tapiero, D.M. Townsend, K.D. Tew, Trace elements in human physiology and pathology, Copper Biomed. Pharmacother. 57 (2003) 386–398, https://doi.org/10.1016/s0753-3322(03)00012-x.
[2] J.W. Chen, T. Zeoli, N.C. Hughes, A. Lane, R.A. Berkman, Copper deficiency myelopathy mimicking cervical spondylitic myelopathy: a systematic review of the literature with case report, Spine J. 24 (11) (2024) 2026–2034.
[3] N. Tahir, A. Ashraf, S.H.B. Waqar, A. Rafae, L. Kantamneni, T. Sheikh, R. Khan, Copper deficiency, a rare but correctable cause of pancytopenia: a review of literature, Expert Rev. Hematol. 15 (11) (2022) 999–1008.
[4] R. Petruzzelli, E. Polishchuk, R. Polishchuk, Copper in human health and disease: insights from inherited disorders, Physiology 10 (2025), https://doi.org/10.1152/physiol.00032.2025.
[5] W.A.M. Ghonimi, M.A.Z. Alferah, N. Dahran, E.S. El-Shetry, Hepatic and renal toxicity following the injection of copper oxide nanoparticles (CuO NPs) in mature male Westar rats: histochemical and caspase 3 immunohistochemical reactivities, Environ. Sci. Pollut. Res. Int. 29 (2022) 81923–81937, https://doi.org/10.1007/s11356-022-21521-2.
[6] R. Mandil, A. Prakash, A. Rahal, S. Koli, R. Kumar, S.K. Garg, Evaluation of oxidative stress-mediated cytotoxicity and genotoxicity of copper and flubendiamide: amelioration by antioxidants in vivo and in vitro, Toxicol. Res. 12 (2023) 232–252, https://doi.org/10.1093/toxres/tfad011.
[7] L. Li, Z. Tai, W. Liu, et al., Copper overload impairs hematopoietic stem and progenitor cell proliferation via prompting HSF1/SP1 aggregation and the subsequently downregulating FOXM1-Cytoskeleton axis, iScience 26 (2023) 106406, https://doi.org/10.1016/j.isci.2023.106406.
[8] L. Lu, Y. Zhang, W. Shi, et al., The role of autophagy in copper-induced apoptosis and developmental neurotoxicity in SH-SY5Y Cells, Toxics 13 (2025), https://doi.org/10.3390/toxics13010063.
[9] S. Lin, J. Cai, Y. Huang, et al., Macrothrombocytopenia with leukocyte inclusions in a patient with Wilson disease: a case report and literature review, BMC Med. Genom. 17 (2024) 188, https://doi.org/10.1186/s12920-024-01960-1.
[10] M. Zhvania, K. Gogberashvili, M. Gagoshidze, E. Uberi, Wilson disease with thrombocytopenia (case report), Georgian Med. N. (2014) 61–64.
[11] G. Bayer, A. Bauvois, J. Mankikian, et al., [Ecchymosis as the presenting manifestation of Wilson disease: a case report], Rev. Med. Interne 38 (2017) 416–419, https://doi.org/10.1016/j.revmed.2016.08.010.
[12] A. Sapuppo, P. Pavone, A.D. Pratico, M. Ruggieri, G. Bertino, A. Fiumara, Genotype-phenotype variable correlation in Wilson disease: clinical history of two

sisters with the similar genotype, BMC Med. Genet. 21 (2020) 128, https://doi.org/10.1186/s12881-020-01062-6.
[13] S. Kanitkar, A. Borle, M. Ahlawat, S.P. Ande, S. Raut, An unusual presentation of Wilson's disease, Cureus 16 (4) (2024) e58407.
[14] H.J. Zhong, P. Xiao, D. Lin, H.M. Zhou, X.X. He, Cirrhosis in Wilson disease is characterized by impaired hepatic synthesis, leukopenia and thrombocytopenia, Int. J. Med. Sci. 17 (10) (2020) 1345–1350.
[15] J. Kalita, V. Kumar, S. Chandra, B. Kumar, U.K. Misra, Worsening of Wilson disease following penicillamine therapy, Eur. Neurol. 71 (3-4) (2014) 126–131.
[16] T. Litwin, A. Antos, J. Bembenek, A. Przybyłkowski, I. Kurkowska-Jastrzębska, M. Skowrońska, A. Członkowska, Copper deficiency as Wilson's disease overtreatment: a systematic review, Diagnostics 13 (14) (2023) 2424.
[17] H.C. Hogland, N.P. Goldstein, Hematologic (cytopenic) manifestations of Wilson's disease (hepatolenticular degeneration), Mayo Clin. Proc. 53 (8) (1978) 498–500. PMID: 682676.
[18] Z. Jian, H. Guo, H. Liu, et al., Oxidative stress, apoptosis and inflammatory responses involved in copper-induced pulmonary toxicity in mice, Aging 12 (2020) 16867–16886, https://doi.org/10.18632/aging.103585.
[19] Y.T. Fan, D.Q. Peng, J.L. Shen, et al., Copper excess induces autophagy dysfunction and mitochondrial ROS-ferroptosis progression, inhibits cellular biosynthesis of milk protein and lipid in bovine mammary epithelial cells, Ecotoxicol. Environ. Saf. 291 (2025) 117783, https://doi.org/10.1016/j.ecoenv.2025.117783.
[20] D. Tao, Y. Wang, J. Liu, R. Chen, M. Qi, S. Xu, Mechanism of CuSO4 cytotoxicity in goat erythrocytes after high-level in vitro exposure to isotonic media, Ecotoxicol. Environ. Saf. 208 (2021 Jan 15) 111730, https://doi.org/10.1016/j.ecoenv.2020.111730. Epub 2020 Dec 9. PMID: 33396061.
[21] R. Sadiq, Q.M. Khan, A. Mobeen, A. Shah, Genotoxicity of aluminium oxide, iron oxide, and copper nanoparticles in mouse bone marrow cells, Arh. Hig. Rada. Toksikol. 72 (2021) 315–325, https://doi.org/10.2478/aiht-2021-72-3578.
[22] I.C. Lee, J.W. Ko, S.H. Park, et al., Comparative toxicity and biodistribution assessments in rats following subchronic oral exposure to copper nanoparticles and microparticles, Part. Fibre Toxicol. 13 (2016) 56, https://doi.org/10.1186/s12989-016-0169-x.
[23] W.H. De Jong, E. De Rijk, A. Bonetto, et al., Toxicity of copper oxide and basic copper carbonate nanoparticles after short-term oral exposure in rats, Nanotoxicology 13 (2019) 50–72, https://doi.org/10.1080/17435390.2018.1530390.
[24] K. Takeuchi, M. Ogura, H. Saito, M. Satoh, M. Takeuchi, Production of platelet-like particles by a human megakaryoblastic leukemia cell line (MEG-01), Exp. Cell Res. 193 (1) (1991) 223–226.
[25] P. Tsvetkov, S. Coy, B. Petrova, M. Dreishpoon, A. Verma, M. Abdusamad, J. Rossen, L. Joesch-Cohen, R. Humeidi, R.D. Spangler, J.K. Eaton, E. Frenkel, M. Kocak, S.M. Corsello, S. Lutsenko, N. Kanarek, S. Santagata, T.R. Golub, Copper induces cell death by targeting lipoylated TCA cycle proteins, Science 375 (6586) (2022) 1254–1261.
[26] L. Chen, J. Min, F. Wang, Copper homeostasis and cuproptosis in health and disease, Signal Transduct. Target Ther. 7 (1) (2022) 378.
[27] N.N. Farshori, M.A. Siddiqui, M.M. Al-Oqail, et al., Copper oxide nanoparticles exhibit cell death through oxidative stress responses in human airway epithelial cells: a mechanistic study, Biol. Trace Elem. Res. 200 (2022) 5042–5051, https://doi.org/10.1007/s12011-022-03107-8.
[28] C. Dey, M. Roy, P. Pal, R. Ghosh, S.G. Dey, Mechanism of oxidative stress and neurotoxicity associated with heme and copper-Aβ relevant to Alzheimer's disease, Chem. Soc. Rev. 54 (20) (2025) 9457–9499.
[29] J. Chen, Y. Yang, F. Yang, X. Gao, G. Hu, Z. Xiong, K.A. Al-Mutairi, L. Yan, J. Li, X. Dai, Copper and vanadium induce oxidative stress and pyroptosis in the duck brain via activating the TLR4/NF-κB-p65 signaling pathway, Biometals 38 (6) (2025) 1731–1745.
[30] B. Witt, S. Friese, V. Walther, F. Ebert, J. Bornhorst, T. Schwerdtle, Cellular mechanisms of copper neurotoxicity in human, differentiated neurons, Arch. Toxicol. 99 (2) (2025) 689–699.
[31] R. Pandey, A.N. Roy, S. Sarkar, R. Rohman, K. Chakraborty, R. Bargakshatriya, S. Pandey, Pruthwiraj, D. Bhattacharya, S. Kumar, S. Maji, A.T. Pezacki, S. K. Pramanik, C.J. Chang, A. Bhattacharjee, N. Sengupta, A. Das, A. Gupta, Repurposing melatonin's therapeutic potential in Wilson disease: addressing copper overload and redox imbalance, Redox Biol. 89 (2025) 103971.
[32] X. Wang, W. Ling, Y. Zhu, C. Ji, X. An, Y. Qi, S. Li, C. Zhang, R. Tong, D. Jiang, B. Kang, Spermidine alleviates copper-induced oxidative stress, inflammation and cuproptosis in the liver, FASEB J. 39 (6) (2025) e70453.
[33] L. Wang, L. Wu, T. Wang, Y. Yue, Z. Jiang, P. Jiang, H. Zhou, L. He, Z. Xia, Y. Song, F. Wang, X. Xiao, H. Han, Melatonin ameliorates copper accumulation-induced cognitive impairment in Wilson disease via activation of the SIRT3/FOXO3α signaling pathway, Neuropharmacology 284 (2026) 110779.
[34] D. Desaulniers, G. Zhou, A. Stalker, C. Cummings-Lorbetskie, Effects of copper or zinc organometallics on cytotoxicity, DNA damage and epigenetic changes in the HC-04 human liver cell line, Int J. Mol. Sci. 24 (21) (2023) 15580.
[35] E. Falcone, F. Stellato, B. Vileno, M. Bouraguba, V. Lebrun, M. Ilbert, S. Morante, P. Faller, Revisiting the pro-oxidant activity of copper: interplay of ascorbate, cysteine, and glutathione, Metallomics 15 (7) (2023) mfad040.
[36] W.A. Ansari, K. Srivastava, M. Nasibullah, et al., Reactive oxygen species (ROS): sources, generation, disease pathophysiology, and antioxidants, Discov. Chem. 2 (2025) 191, https://doi.org/10.1007/s44371-025-00275-z.
[37] S. Anwar, T. Sarwar, A.A. Khan, A.H. Rahmani, Therapeutic Applications and Mechanisms of Superoxide Dismutase (SOD) in Different Pathogenesis, Biomolecules 15 (8) (2025) 1130.
[38] F. Lairion, C. Saporito-Magrina, R. Musacco-Sebio, J. Fuda, H. Torti, M.G. Repetto, Nitric oxide, chronic iron and copper overloads and regulation of redox homeostasis in rat liver, J. Biol. Inorg. Chem. 27 (2022) 23–36, https://doi.org/10.1007/s00775-021-01908-1.
[39] S. Kumar, Caspase function in programmed cell death, Cell Death Differ. 14 (1) (2007) 32–43.
[40] S. Santos, A.M. Silva, M. Matos, S.M. Monteiro, A.R. Alvaro, Copper induced apoptosis in Caco-2 and Hep-G2 cells: Expression of caspases 3, 8 and 9, AIF and p53, Comp. Biochem. Physiol. C. Toxicol. Pharmacol. 185-186 (2016) 138–146, https://doi.org/10.1016/j.cbpc.2016.03.010.
[41] H. Liu, H. Guo, Z. Jian, et al., Copper induces oxidative stress and apoptosis in the mouse liver, Oxid. Med. Cell Longev. 2020 (2020) 1359164, https://doi.org/10.1155/2020/1359164.
[42] W.S. Sarawi, A.M. Alhusaini, L.M. Fadda, et al., Curcumin and nano-curcumin mitigate copper neurotoxicity by modulating oxidative stress, inflammation, and Akt/GSK-3beta signaling, Molecules 26 (2021), https://doi.org/10.3390/molecules26185591.
[43] A. Hamacher-Brady, N.R. Brady, Mitophagy programs: mechanisms and physiological implications of mitochondrial targeting by autophagy, Cell Mol. Life Sci. 73 (4) (2016) 775–795.
[44] S. Rao, M. Skulsuppaisarn, L.M. Strong, X. Ren, M. Lazarou, J.H. Hurley, G. Hummer, Three-step docking by WIPI2, ATG16L1, and ATG3 delivers LC3 to the phagophore, Sci. Adv. 10 (6) (2024) eadj8027.
[45] T. Johansen, T. Lamark, Selective autophagy mediated by autophagic adapter proteins, Autophagy 7 (3) (2011) 279–296.
[46] X. Huang, L. Liu, J. Yao, C. Lin, T. Xiang, A. Yang, S-acylation regulates SQSTM1/p62-mediated selective autophagy, Autophagy 20 (6) (2024) 1467–1469 (d).
[47] S. Pantoom, A. Pomorski, K. Huth, C. Hund, J. Petters, A. Krężel, A. Hermann, J. Lukas, Direct interaction of ATP7B and LC3B proteins suggests a cooperative role of copper transportation and autophagy, Cells 10 (11) (2021) 3118.
[48] S. Tang, C. Liang, W. Hou, Z. Hu, X. Chen, J. Zhao, W. Zhang, Z. Duan, L. Bai, S. Zheng, ATP7B R778L mutant hepatocytes resist copper toxicity by activating autophagy and inhibiting necroptosis, Cell Death Discov. 9 (1) (2023) 344.
[49] Z. Kang, N. Qiao, G. Liu, H. Chen, Z. Tang, Y. Li, Copper-induced apoptosis and autophagy through oxidative stress-mediated mitochondrial dysfunction in male germ cells, Toxicol. Vitr. 61 (2019) 104639.
[50] P. Xu, M. Cao, X. Dong, et al., Nanosized copper particles induced mesangial cell toxicity via the autophagy pathway, Braz. J. Med. Biol. Res. 55 (2022) e12252, https://doi.org/10.1590/1414-431X2022e12252.
[51] L. Lu, Y. Zhang, W. Shi, Q. Zhou, Z. Lai, Y. Pu, L. Yin, The role of autophagy in copper-induced apoptosis and developmental neurotoxicity in SH-SY5Y cells, Toxics 13 (1) (2025) 63.

## Glossary

*SOD:* superoxide dismutase
*WD:* Wilson disease
*ROS:* reactive oxygen species
*TEM:* transmission electron microscopy
*PI:* propidium iodide
*PBS:* phosphate-buffered saline
*MDA:* malondialdehyde
*TBA:* hiobarbituric acid
*ER:* endoplasmic reticulum